

An Empirical Study of a Photovoltaic Module's Performance Under Real-World Environmental Conditions

Ryan Xin

ABSTRACT

This study presents the design, implementation, and empirical analysis of a field data acquisition system used to characterize a polycrystalline photovoltaic (PV) module under real-world environmental conditions. Phase I comprised a 6-day monitoring campaign using a fixed 150 Ω load; Phase II comprised rapid load-sweep experiments (20–200 Ω) to derive the module's I–V and P–V characteristic curves and identify maximum power points (MPPs). The results quantify the dominant role of irradiance on power output, demonstrate the negative thermal coefficient of the module's voltage and power, and reveal a significant mismatch loss between fixed-load operation and the dynamic MPP. These findings emphasize the importance of deploying Maximum Power Point Tracking (MPPT) for practical PV systems.

KEYWORDS

Photovoltaic, I–V curve, P–V curve, Maximum Power Point (MPP), irradiance, temperature, MPPT, field experiment

1. INTRODUCTION

Photovoltaic (PV) modules are widely used in distributed renewable energy systems. However, laboratory Standard Test Conditions (STC) often fail to capture the temporal variability experienced in the field: changing irradiance, temperature fluctuations, and partial shading can alter the operating point and energy yield substantially [1],[5]. The objectives of this work are to (1) build a robust field data logger capable of multi-sensor acquisition, (2) quantify the dependencies of module power on irradiance and temperature under a fixed load, (3) empirically derive I–V and P–V curves using a rapid resistor-sweep method, and (4) quantify the energy lost by operating at a fixed load compared to the time-varying MPP.

2. SYSTEM DESIGN AND METHODOLOGY

2.1 Hardware

- Controller: TTGO T8 (ESP32).
- PV module: 10 W polycrystalline module ($V_{oc} \approx 21$ V).
- Power measurement: INA226 high-side current and power sensor.
- Irradiance measurement: MAX44009 ambient light sensor (lux).
- Module temperature: $2 \times$ DS18B20 waterproof probes attached on the panel rear.
- Ambient sensing: BMP280 (temperature, pressure).
- I²C multiplexer: TCA9548A.
- Data storage: MicroSD card module.
- UI: SSD1306 OLED for local status.

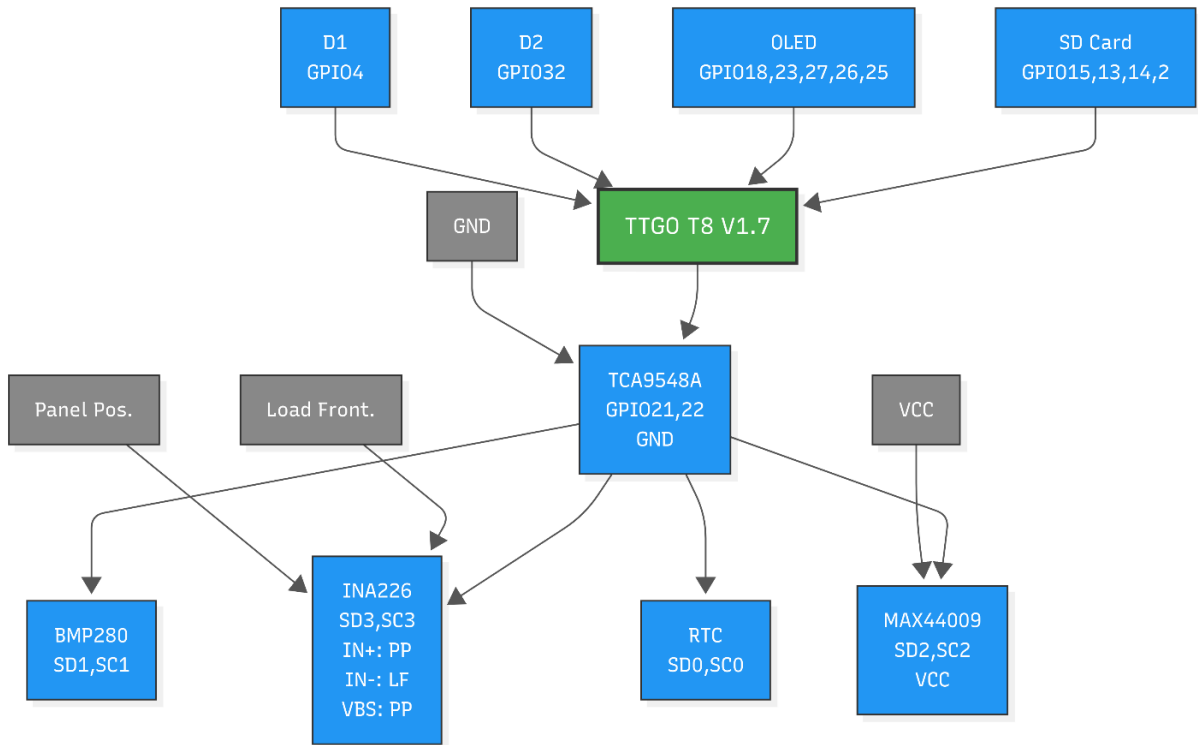


Fig. 1 System architecture showing the TTGO T8 controller, sensors, power measurement path, and storage.

The experimental setup followed general guidelines consistent with international PV performance testing protocols [4].

2.2 Firmware and Data Logging

Firmware was implemented in Arduino C++ and designed to be fault-tolerant. Critical subsystems (SD card, RTC) are initialized with indefinite retries; sensors have finite retry logic. Data were sampled at nominal intervals of ≈ 30 s and logged to CSV with a timestamp. Logged fields include: timestamp, panel voltage (V), current (A or mA), computed power (W), panel_temp_1_C, panel_temp_2_C, ambient_temp_C, light_lux, and other relevant status flags.

2.3 Experimental Procedure

Phase I—Fixed load: A $150\ \Omega$ power resistor served as the fixed resistive load. The system captured continuous measurements over 6 days covering a range of weather conditions (clear, partially cloudy, rainy). The dataset produced time series suitable for diurnal energy integration and correlation analysis.

Phase II—Load sweeps: Rapid manual resistor sweeps were performed using resistors from $200\ \Omega$ down to $20\ \Omega$. This range was chosen to span the panel's expected optimal load resistance, which was theoretically estimated to be around $30\ \Omega$, thereby ensuring the capture of the MPP.

3. DATA PROCESSING AND QUALITY CONTROL

3.1 Loading and structural correction

CSV files were read with robust encoding handling. For Phase II, merged-resistance labels were forward-filled so every data row had an associated Resistance_Ohm. Separator rows were dropped.

3.2 Error removal and unit normalization

Known DS18B20 error values (85.0 °C) were removed. All numeric columns were cast to appropriate units: Voltage in V, Current in A (convert from mA where necessary), Power in W (convert from mW where necessary). Panel_Temp_Avg_C was computed as the mean of the two DS18B20 sensors.

3.3 Feature engineering

Derived columns included: Power_W, Panel_Temp_Avg_C, and sample elapsed time for intra-block time series analysis. Per-block aggregation produced mean_voltage_V, mean_current_A, mean_power_W, mean_light_lux, and mean_panel_temp_C. Summary CSVs (`daily_summary.csv` and `blocks_summary.csv`) were produced at the end of the processing pipeline.

4. RESULTS

4.1 Phase I — Fixed $150\ \Omega$: time-series and baseline behavior

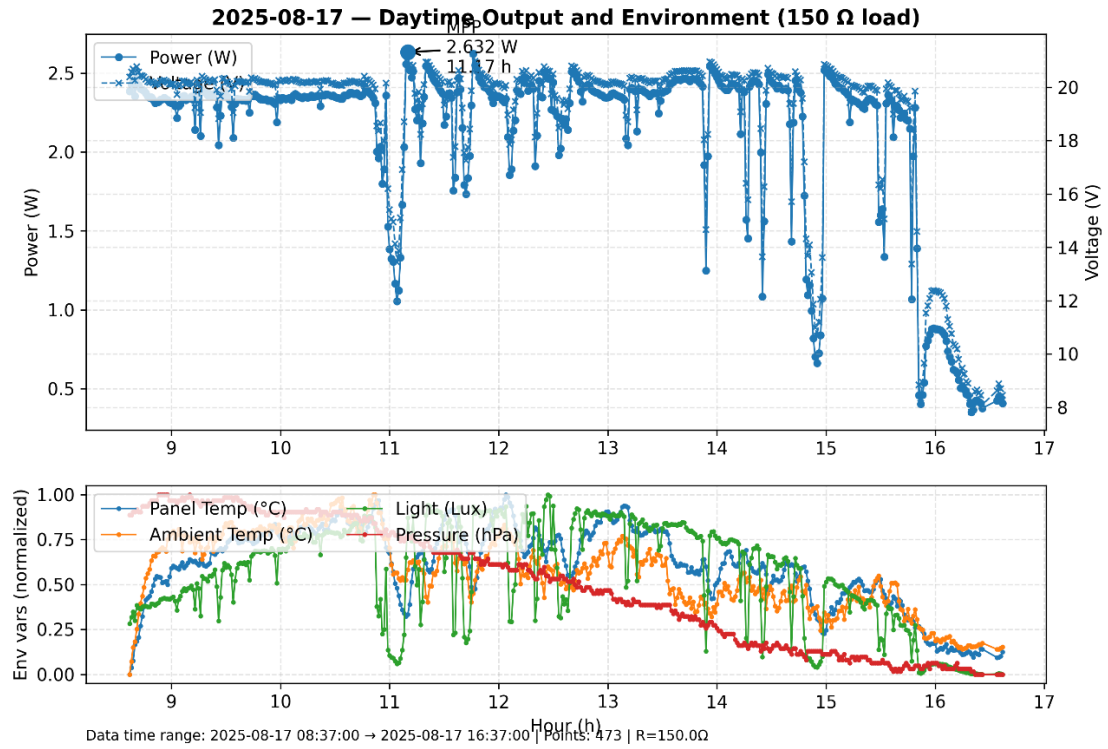


Fig. 2 A representative record of panel irradiance (lux), panel temperature ($^{\circ}\text{C}$), and measured power (W) under a fixed $150\ \Omega$ load in a day time series.

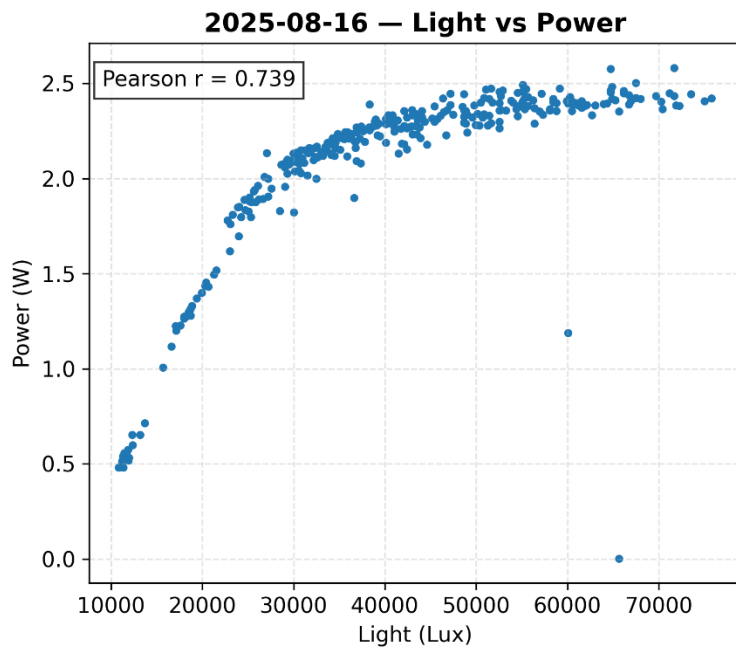


Fig. 3 Correlation between power and light in the day suggests high relevance.

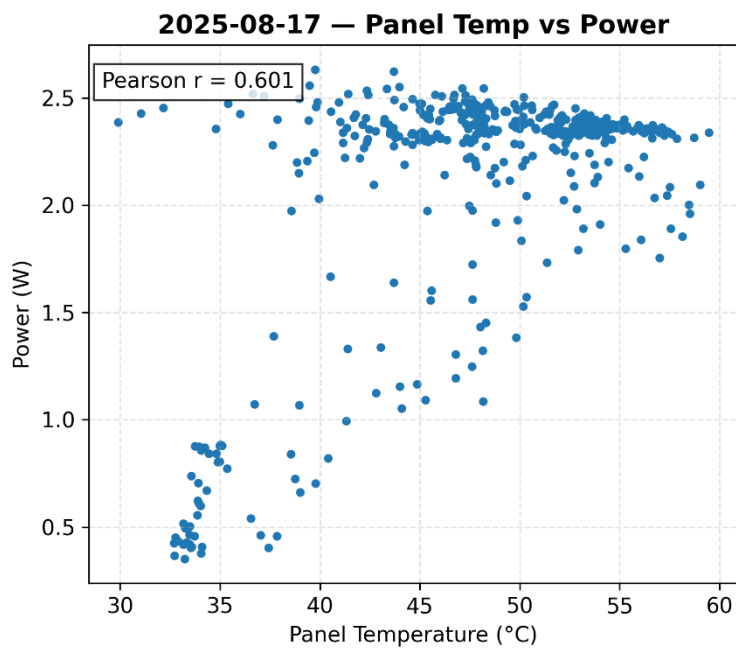


Fig. 4 Lower panel temperature presents slight improvement to the power, especially when power is greater than 2.0W.

Correlation analysis:

- **Pearson Correlation** between light (lux) and power (W) is high (r in range 0.739 to 0.918).
- Efficiency vs Panel Temperature diagrams show that with panel generating low power, the negative effect of panel temperature on power is not evident. But if the power generated is above a certain threshold, this effect would exist.

4.2 Phase II — Single Load-Switch Characterization

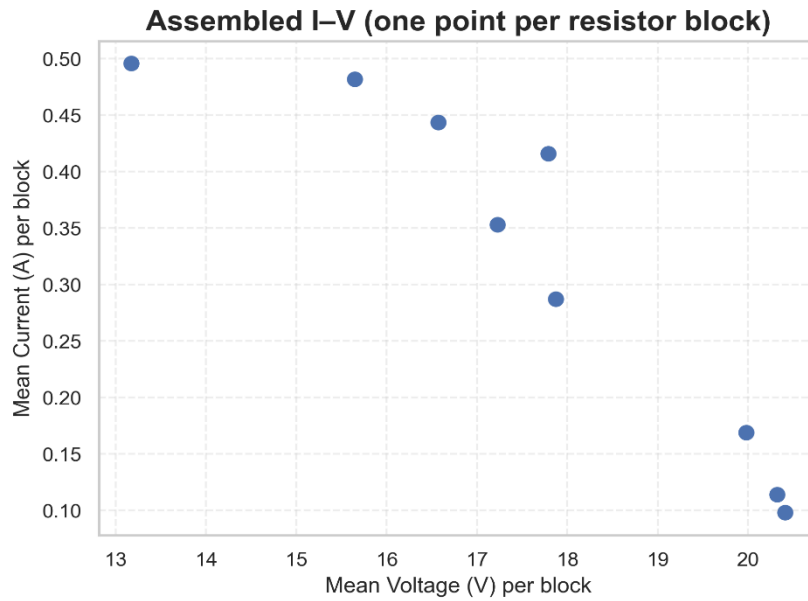


Fig. 5 Voltage and current response during sequential resistor switching. Each point corresponds to a different fixed load.

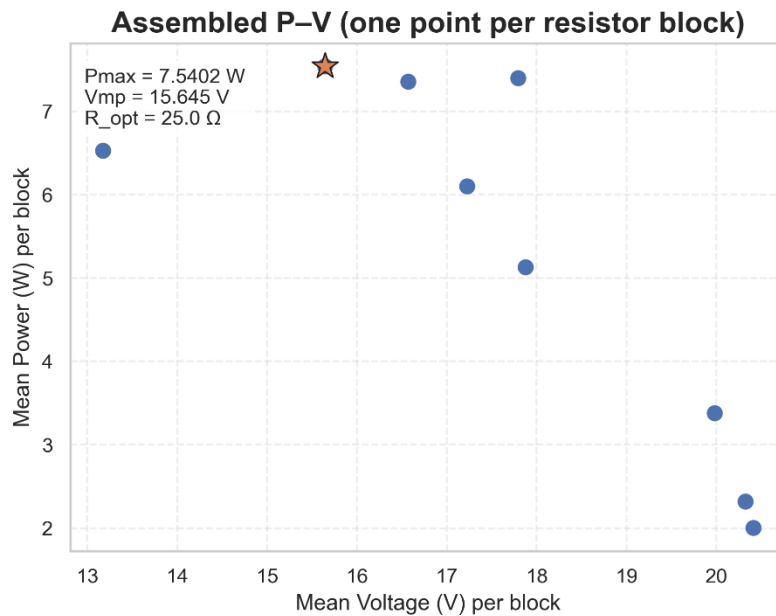


Fig. 6 Power–voltage curve for the sweep. The maximum power point (MPP) is indicated with a star marker at coordinates (Vmp, Pmax) [2].

Observations:

- Clear voltage collapse was observed under low-resistance conditions ($\leq 30 \Omega$), consistent with current limitation of the panel under the irradiance present during the test.
- At intermediate loads ($\approx 100\text{--}150 \Omega$), the panel maintained higher voltage while still delivering non-negligible current, leading to a broad region of near-maximum power.
- The effective optimal load (R_{opt}) during this session was approximately 25Ω , with a corresponding power of 7.54W , under irradiance of 93250 lux .

4.3 Mismatch loss: fixed load vs MPP

Instantaneous Mismatch Loss: This metric represents the relative power loss at a specific moment in time by comparing the power generated by the fixed 150 Ω load against the true maximum power potential (MPP) of the panel under nearly identical irradiance conditions. It is calculated as:

$$\text{Mismatch Loss (\%)} = \frac{P_{\text{MPP}} - P_{\text{measured}}}{P_{\text{MPP}}} \times 100\%$$

where P_{MPP} is the maximum power found during a Phase II load sweep, and P_{measured} is the power measured at the 150 Ω load from a Phase I sample under similar environmental conditions.

Conservative Daily Energy Loss: This metric provides an upper-bound estimate of the total energy not harvested over a full day due to the use of the fixed load. It compares the total energy actually produced with a theoretical maximum. The daily energy (E) is calculated by the trapezoidal integration of the power ($P(t)$) time series over the sunlit hours (t_{start} to t_{end}). The loss is then:

$$\text{Daily Loss (\%)} = \frac{E_{\text{theoretical}} - E_{\text{measured}}}{E_{\text{theoretical}}} \times 100\%$$

where $E_{\text{measured}} = \int_{t_{\text{start}}}^{t_{\text{end}}} P_{150\Omega}(t) dt$, and the theoretical energy is estimated as $E_{\text{theoretical}} = P_{\text{max}} \times (t_{\text{end}} - t_{\text{start}})$

To quantify the operational penalty of using a non-optimal fixed load, the energy yield under the 150 Ω resistor was compared against a theoretical maximum. The maximum power measured during a high-irradiance sweep in Phase II was **$P_{\text{max}} = 7.54 \text{ W}$** . In contrast, a data point from Phase I under nearly identical irradiance conditions ($\sim 93,000 \text{ lux}$) yielded only **$P_{150} = 2.34 \text{ W}$** . This results in an **instantaneous mismatch loss of 69.0%**.

To estimate the cumulative effect over a full day, the total energy harvested on a representative clear day with the 150 Ω load was calculated via trapezoidal integration of the power time series, yielding **4.06 Wh**. A theoretical maximum daily yield was then estimated by assuming the peak power ($P_{\text{max}} = 7.54 \text{ W}$) was constantly available during the same sunlit hours. This comparison results in a theoretical maximum yield of **24.51 Wh**, suggesting a **conservative daily energy loss of approximately 83.4%**. While this

assumption represents an idealized upper bound, it starkly illustrates the substantial magnitude of energy forfeited by not operating at the MPP

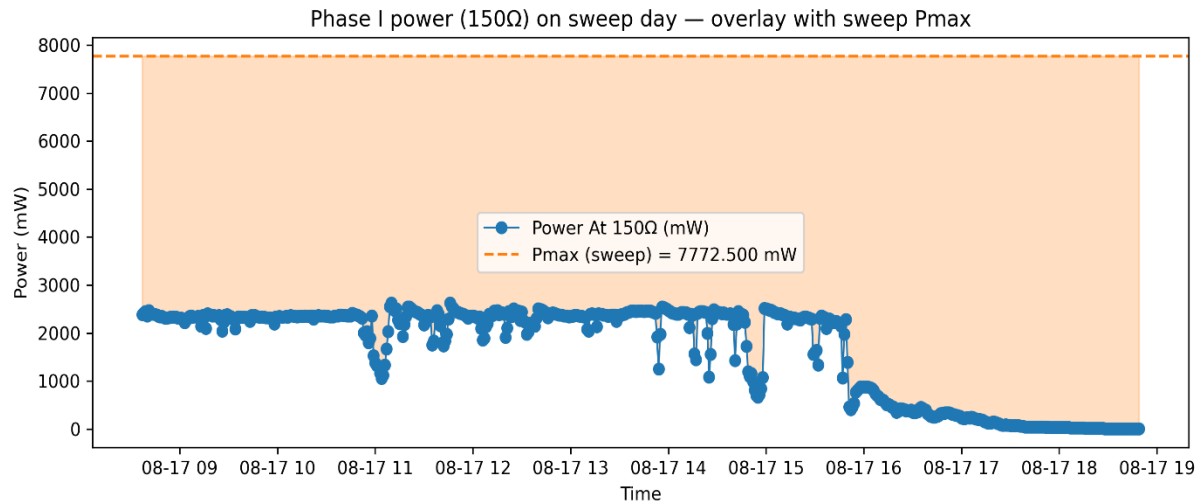


Fig. 7 Theoretical Pmax (blue) vs actual P at 150 Ω (orange) for a representative clear day. Shaded area indicates energy lost by fixed-load operation.

5. DISCUSSION

The most compelling finding of this study is the quantification of the substantial energy mismatch loss—as high as 83.4% on a representative day—when operating the PV module with a simple fixed resistor versus its true Maximum Power Point. This result moves beyond theoretical understanding and provides strong empirical evidence for the indispensable role of MPPT technology in practical PV applications [2].

The strong positive Pearson correlation ($r > 0.73$) between irradiance and power output confirms that irradiance is the primary driver of power generation. However, the scattering of data points around the regression line indicates that other variables are simultaneously influencing the output, preventing a perfectly linear relationship.

This study successfully isolated the negative thermal coefficient of the module [3]. As

observed in Figure 4, at higher power levels (i.e., high irradiance), increasing panel temperatures clearly suppress the maximum achievable power. This is consistent with semiconductor physics, where elevated temperatures increase carrier recombination rates and reduce the cell's open-circuit voltage, thereby lowering overall efficiency.

The empirically derived P-V curve (Figure 6) provides a clear 'performance fingerprint' of the module under specific conditions. The identification of an optimal load resistance ($R_{opt} \approx 25\Omega$) far from our fixed test load (150Ω) is the direct cause of the observed mismatch loss. Furthermore, by comparing sweeps from different times of day, we observed that the MPP is not static; it shifts with irradiance, underscoring the challenge that MPPT controllers are designed to solve.

Several limitations should be acknowledged. The manual load-scanning process, while effective, introduces a small time delay between measurements, during which irradiance could slightly fluctuate. An automated electronic load would provide more consistent sweeps. Additionally, the MAX44009 sensor measures illuminance (lux), which is not a perfect proxy for the full spectrum solar irradiance (W/m^2); however, it provides a strong and consistent relative measure for this study's purposes.

6. CONCLUSION

This work successfully demonstrated a field-based methodology for the complete characterization of a PV module. Through a two-phase experiment, this study (1) confirmed the dominant, positive correlation of irradiance with power, (2) quantified the negative impact of operating temperature on efficiency, and (3) most importantly, empirically measured the substantial energy mismatch losses (up to 83.4%) caused by fixed-load operation. The results provide a powerful, data-driven justification for the necessity of MPPT in maximizing energy yield from photovoltaic systems.

REFERENCES

- [1] W. De Soto, S. A. Klein, and W. A. Beckman, “Improvement and validation of a model for photovoltaic array performance,” *Solar Energy*, vol. 80, no. 1, pp. 78–88, 2006, doi: 10.1016/j.solener.2005.06.010.
- [2] T. Eswam and P. L. Chapman, “Comparison of photovoltaic array maximum power point tracking techniques,” *IEEE Transactions on Energy Conversion*, vol. 22, no. 2, pp. 439–449, 2007, doi: 10.1109/TEC.2006.874230.
- [3] E. Skoplaki and J. A. Palyvos, “Operating temperature of photovoltaic modules: A survey of pertinent correlations,” *Renewable Energy*, vol. 34, no. 1, pp. 23–29, 2009, doi: 10.1016/j.renene.2008.04.009.
- [4] International Electrotechnical Commission, *IEC 61853-1: Photovoltaic module performance testing and energy rating — Part 1: Irradiance and temperature performance measurements and power rating*. Geneva, Switzerland: IEC, 2011.
- [5] J. A. Duffie and W. A. Beckman, *Solar Engineering of Thermal Processes*, 3rd ed. Hoboken, NJ, USA: Wiley, 2006.